Robot-Assisted Retraction for Transoral Surgery

Lifeng Zhu, *Associate Member, IEEE*, Jiangwei Shen, Shuyan Yang, and Aiguo Song, *Senior Member, IEEE*

***Abstract*—Tissue retraction is an important task in head and neck surgery to leave space for surgical operations. Because the contact between the retractor and soft tissue is not trivial to model, the retraction operation has not been well addressed by robots in modern robot-assisted surgery. We propose a human-robot collaboration approach to assist the retraction for transoral surgery. The surgeons only need to roughly place the retractors into the oral cavity and specify the recommended retraction force. Robot manipulators will automatically retract the tissues in a safe way. In order to keep the touching force safe, we employ a force-sensing system at the distal end of the retractor. By analyzing the real-time force sensor data, we propose a control strategy which combines active retraction angle compensation and passive torque compensation to adjust the retractor, further reducing potential slippage during the retraction. The proposed method ensures the retraction is adaptive to unknown perturbations of the human anatomy. Our system requires no extra recognition or calibration of the surgical scene or the human tissue models. The approach is validated with two robot manipulators and force-sensing retractors on a physical head phantom as well as a cadaveric experiment. We show that the robots stably retract the mouth under various configurations, where the relative error of the stable retraction force does not exceed 11.8%.**

***Index Terms*—Medical robots and systems, robot-assisted retraction, transoral surgery.**

I. Introduction

DURING surgical procedure, retraction plays an essential role in optimizing the surgical vision field [1]. In conventional transoral surgery, a mechanical gag is required to fix the retraction before surgery which is complicated to install and inflexible to adjust [2]. Alternatively, a surgical assistant should be occupied with manually holding the retractor for exposing the operation field. Maintaining the same posture for a long time is likely to cause physical fatigue. It is also risky to the patient, especially for a long surgery. Effective communication between the assistant and the surgeon needs to be maintained at all times, neither being able to fully concentrate on their immediate surgical task [3]. A robot-assisted retraction solution may significantly benefit surgeons, assistants, and patients.

Manuscript received 9 August 2022; accepted 8 September 2022. Date of publication 3 October 2022; date of current version 13 October 2022. This letter was recommended for publication by Associate Editor F. Alambeigi and Editor J. Burgner-Kahrs upon evaluation of the reviewers' comments. This work was supported in part by the NSFC under Grants 62133009 and 92148205, in part by the Natural Science Foundation of Jiangsu Province under Grant BK20211159 and in part by the Fundamental Research Funds for the Central Universities.

The authors are with the State Key Laboratory of Bioelectronics, Jiangsu Key Lab of Remote Measurement and Control, School of Instrument Science and Engineering, Southeast University, Nanjing 210096, China (e-mail: lfzhulf@gmail.com; 220203611@seu.edu.cn; 220193280@seu.edu.cn; a.g.song@seu.edu.cn).

Digital Object Identifier 10.1109/LRA.2022.3211491

With the success of surgical robots, surgeons expect to distribute tedious and laborious tasks to robots and focus on more advanced operations [4]. Tissue retraction in transoral surgery is one of such low-level tasks. However, it is not easy to make surgical robots safely retract the tissues. While many methods for robot manipulation of flexible objects have been proposed, successful applications assume good models of the interaction with the environment. In practice, it is costly to precisely reconstruct the human anatomy and its material properties. Therefore, for robot-assisted retraction based on computer vision [5], [6], it is challenging to track the deformation of, e.g, the mouth tissues inside the oral cavity during the transoral surgery. On the other hand, limited by the generalization ability, existing learning-based research [7], [8] is also hard to deploy in an open surgical environment.

We introduce to use force-sensing data online [9] for controlling the retractors. Interactive control techniques such as impedance control are developed to deal with deformable objects in recent years [10]. However, for the task of tissue retraction in transoral surgery, there are still many challenging problems. First, it is hard to measure the deformation of the tissue, which is commonly incorporated in interaction control [11]. Besides, the contact region between the manipulator and soft object is usually assumed to be known and fixed in the compliance control [12], while the slippage is unavoidable during retraction. Successful control of soft objects may also require a reliable simulation of the tissues [13], which is commonly not available for transoral surgery in an open environment. Furthermore, surgeons may frequently adjust the pose of the retractor before they stably hold it during the retraction. It is not a linear motion and we cannot directly apply force control for this process. To the best of our knowledge, it is not known how to model the retraction process in a transoral surgery with compliance control. Especially for individuals with unknown different tissue models, it is not clear whether robot-assisted retraction will ensure a safe surgery.

In this work, we propose a human-robot collaboration approach to facilitate the retraction task and check its applicability to transoral surgery. We provide an interface to allow surgeons to roughly pose the retractors before the retraction. By introducing a force-sensing system to sense the contact between the distal end of the retractor and the tissues, a force control model is used to leverage the online force signals with the dynamics of the retractor for transoral surgery. The robot will automatically update the pose of the retractor and adjust the retraction distance to respond to random perturbations of the tissues. To improve the contact status between the retractor and tissues, we analyze the sensed force signals and design a passive torque compensation to model the compliance of the retractor. Besides, we propose

an active retraction angle compensation method to reduce slippage on the tissue. Physical experiments on head phantoms are designed and carried out to validate the proposed control.

As the main contributions of this work, we answer the question of whether robot-assisted retraction without pre-surgery tissue modeling is possible for transoral surgery in an open environment. Our technical contribution includes:

1) a human-robot collaboration approach to enable robot-assisted retraction for transoral surgery,
2) a novel control strategy to intelligently update the orientation of the retractor for reducing retraction slippage,
3) comparison of the robotic system to manual retractions and validate our method with a cadaveric experiment.

II. Related Works

Retraction in Robot-assisted Surgery: Advanced robot techniques enable many tasks in surgery completed by robots. Typical operations such as holding the endoscope or controlling forceps are successfully taken by robots, benefiting various surgeries in terms of reducing the workload of surgeons and the risks of precise operations [15]. For tissue retraction, existing work includes designing sensors for the retraction tasks in laparoscopic surgery [16] or neurosurgery [17] and designing new structure of the retractors for abdominal surgery [18], [19]. For transoral surgery, retractors are usually designed to be fixed on the mouth [14] to support robot-assisted surgery. However, the retraction status is not flexible. It takes time to carefully position the static retractor and patients may have mucosal damage to keep the mouth wide open for a long time.

Control Schemes for Robot-assisted Retraction: Robot-assisted retraction has also been studied mostly for laparoscopic surgery [20], while in the early work, the robot only statically holds the retractor and does not consider controlling the force and motion. Most existing methods of robot-assisted retraction are built on a simulation model of the tissues to be retracted [21], [22]. These methods require an accurate three-dimensional model of the tissues, which is challenging to obtain in real-world surgeries. The shape of the anatomy is also observed and analyzed using the vision from endoscopes or cameras [5], [6]. However, because of the complex structure of human anatomy and occlusions in retraction, modeling the dynamics of anatomy from computer vision is not a well-solved problem and it is still not reliable to leave the retraction task to a robot. Recent advances in machine learning are considered in robot-assisted retraction. Pore et al. propose to use reinforcement learning [7] and learning from demonstrations [8] for robot-assisted retraction. The learning-based methods rely on sufficient training data with good quality and suffer from the generalization problem, which is also not ideal for surgery in the open environment.

Compliance Control for Manipulating Soft Objects: Compliance control including force and/or motion control has been studied for manipulating soft objects. For example, impedance or admittance control [24] can produce contact with a desired impedance [25]. Because it is difficult for modeling the desired impedance in manipulating general soft objects, variable impedance control has been proposed to adjust the coefficients by, e.g., learning-based methods [26], [27]. Model-predictive control has also been used for manipulating soft objects [28], [29]. These methods may work well with a good predictive model, which is not easy to build for manipulating soft objects like human tissues. Combining force control with vision data is another direction in manipulating soft objects [30], [31], which demands a reliable vision model to improve performance.

III. Retraction Model

A. Design Factors

The goal of this work is to employ surgical robots to replace surgical assistants for the task of tissue retraction in transoral surgery. We consider the following factors in our design: 1) The surgeon needs to adjust the retraction frequently during the procedure. 2) The retraction needs to remain stable so that operations such as cutting and ablation will not make the retraction unstable. 3) In case large perturbations occur, the retractor should adjust its posture accordingly to avoid damaging the tissue. We analyze the manual retraction process and then design a human-robot collaboration approach to enable robot-assisted retraction. Specifically, we model the retraction task into the following phases as illustrated in Fig. 1.

B. Retraction Phases

Initialization Phase (Phase I): First, the retractors should be sent into the oral cavity and adjust their orientation so that the blade of the retractor roughly faces the tissues to be retracted. As an initialization of our system, we suggest to enable the free drive mode of the robot manipulator. In this way, the retractor as the end-effector will be roughly dragged by the surgeon to an initial pose to start the retraction.

Active Retraction Phase (Phase R): The manipulator starts to actively move the retractor until the update of the surgical cavity is satisfactory to the surgeon. As its representation in the control system, we use a force to quantify the magnitude of retraction. The recommended force is set according to the surgeon's needs, and the manipulator moves along the normal direction of the retractor until the contact force reaches the target value.

Stable Retraction Phase (Phase S): Surgeon operations can cause slight displacement of the tissues. Meanwhile, the manipulator should perform a brief yielding in the procedure of being disturbed, and then resume stable retraction. At the same time, yielding to torque perturbation is also necessary. The robot should also be controlled online in this phase.

Retracting Compensation Phase (Phase C): If the initial orientation is not well aligned with the contact region, undesirable torque between the retractor and the tissue may be too large, causing potential slippage and risk the retraction. In manual retraction, operators sense the retraction status and may retreat to adjust the pose for the next trial. We model this behavior as a retraction compensation phase. In our robot-assisted retraction, the manipulator will back to a non-contact state and compensate for the orientation before its next trial of retraction.

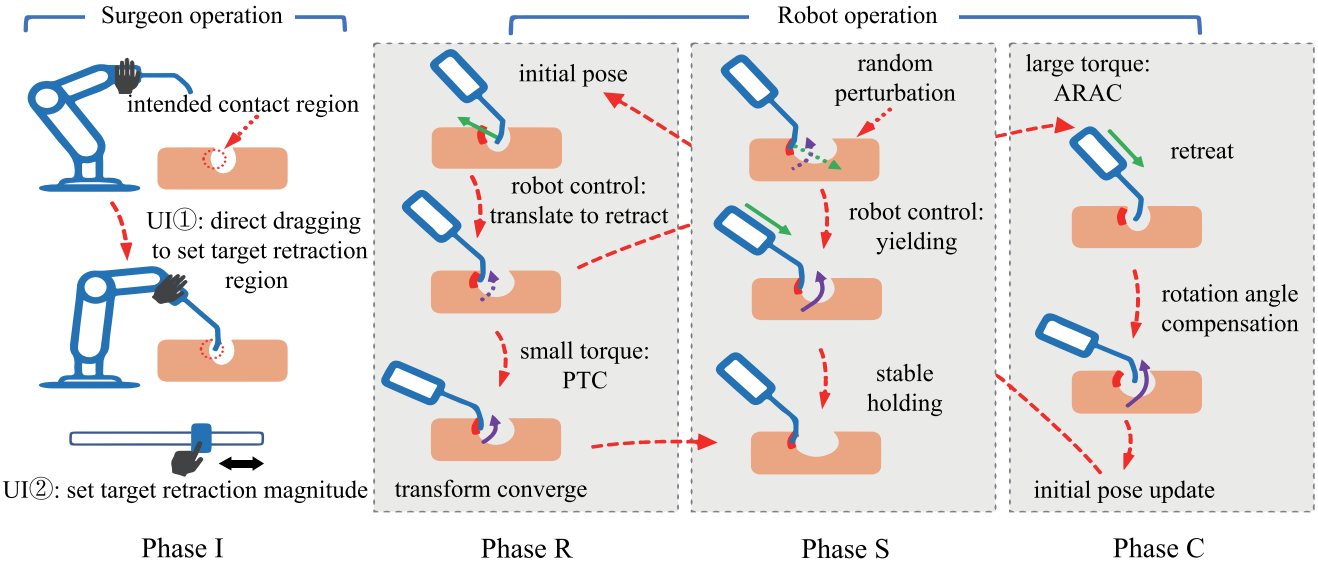

Fig. 1. Overview of the human-robot collaboration control system and retraction phases. The green/purple dotted lines indicate the desired force/torque compensation, and the green/purple solid lines indicate the actual force/torque compensation.

C. Human-Robot Collaboration

Based on the modeled retraction phases, we design a human-robot collaboration approach for the robot-assisted retraction. Because the surgeon is in the loop in transoral surgery, he/she may frequently switch the operation sites. It is not suitable to have the robot automatically guide the retraction without input from surgeons. We, therefore, distribute the high-level task of specifying the intended retraction region and magnitude to the surgeon. The robot takes the low-level task to control the retraction toward the specified contact region with a safe contact. In our human-robot interface, the surgeon drags the manipulators to an initial pose by facing the retractor to the target retraction region. Then the robot will take the active retraction phase to automatically move and hold the retractor. After stabilization, if the surgical field is not satisfactory to expose the operation sites, the surgeon is allowed to adjust the retraction force online to control the retraction magnitude. The surgeon can also pause the system at any time and re-drag the manipulators to complete another surgical subtask. In addition, we set a safety guard for the movement of the manipulator. If the retractor moves out of this limit, the system will stop and remind the surgeon to check the surgical environment. Furthermore, we set the maximum retraction force threshold to ensure safety. It does not exceed 200% of the reference force. In practice, this dangerous situation did not occur in our experiments.

IV. Retraction Control

A. Force-Sensing Retractor

The force signals are essential in our retraction control. Although force sensors installed at the wrist of robot manipulators are more accessible, the estimated contact from the wrist force measurements, which is known as intrinsic contact, is not reliable [32]. In our system, we adopt the force-sensing system

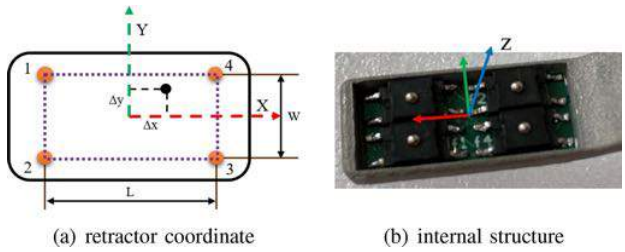

Fig. 2. The force-sensing system. (a) Four force-sensing elements drawn as orange dots provide their pressing forces and are used to compute the resultant force along the normal direction. (b) Close-up view of the sensor assembly.

proposed in our previous work [9], which can be installed at the distal end of the retractor. Fig. 2 shows the structural design of the sensory system. We embed an array of four piezoresistive elements inside the blade region of the retractor. Suppose the pressing forces on the four elements are $F_i, i = 1, 2, 3, 4$, we measure the resultant force F_s applied on the blade of the retractor along the normal direction as

$$F_s = F_1 + F_2 + F_3 + F_4 \tag{1}$$

Different from previous work [9], we add four force signals as inputs to the control system. Furthermore, in combination with the known distances between the force-sensing elements W and L, we further use the four-way force signals to extract the resultant torque on the retractor with respect to the center of mass of the force-sensing system

$$M_x = (F_1 + F_4 - F_2 - F_3)W/2 \tag{2}$$

$$M_y = (F_3 + F_4 - F_1 - F_2)L/2 \tag{3}$$

In this way, the force-sensing information can be extended to three dimensions. This includes the force along the z-axis F_s, and the torques about the x, y direction M_x, M_y. We use the torques in *Phase S* and details will be provided in IV-C.

B. Active Retraction Control

The input entries in the active retraction phase are the contact force signals. In order to distribute our system to an unknown environment without modeling soft tissues, we choose to apply force control on the manipulator. The controller in [23] is employed in this study.

In general, the dynamics of the manipulator in joint space contains $\tau = M(q)\ddot{q} + C(q,\dot{q}) + G(q)$, where $\ddot{\mathbf{q}}, \dot{\mathbf{q}}, \mathbf{q} \in R^n$ are joint space acceleration, velocity, and position, $M(\mathbf{q}) \in R^{n\times n}$, $C(\mathbf{q},\dot{\mathbf{q}}) \in R^n$ and $G(\mathbf{q}) \in R^n$ are the joint space inertia, Coriolis and gravity items. Under the control law $\tau = J^T(\mathbf{q})\mathbf{f}$, where J constitutes the end-effector Jacobian and $\mathbf{f}$ represents the end-effector force in the world space. We simplify the system by dropping non-linear, velocity-dependent terms and gravity-induced acceleration, and obtain

$$\ddot{\mathbf{q}} = M^{-1}J^T\mathbf{f}, \tag{4}$$

which relates $\mathbf{f}$ to instantaneous joint acceleration $\ddot{\mathbf{q}}$, as the centerpiece of the force control scheme. Inputs to the force controller include the reference force F_d and the sensed force F_s collected by the retractor. The error between them is transformed by a PD controller and entered into equation (4). The parameters k_p, k_d in the PD controller determine the dynamic response and stabilization of the retraction. In this way, we get the joint acceleration $\ddot{q}$ of the manipulator as the control command to the manipulator.

C. Stable Retraction

In this phase, the manipulator is still controlled by equation (4). When a random perturbation is applied, the sensed force will change in response and update the error in the controller. The manipulator will move accordingly to align the contact force with the reference force. For the rotational component, the manipulator is regarded to take a passive torque compensation (PTC) here. However, for the retraction task, we find two problems by directly applying the conventional force control scheme in the stable retraction phase.

First, in *Phase S*, the reference force is along the normal direction of the retractor and its magnitude is input by the surgeon. The ideal contact torque is expected to be zero. However, due to the complex deformation and friction, the contact torque does not vanish. If we set the reference torque to zero, the manipulator will continuously rotate and shake the retractor in the stable retraction phase. Considering the contact torque does not vanish in manual retraction as well, we, therefore, set a cutoff value for the reference torque. In practice, we normally find that compensation is not needed for contact torques less than $0.5N \cdot \text{mm}$.

Another problem in the stable retraction is from the inappropriate initial setting, as shown in Fig. 3. When the initial orientation is not well aligned with the tissue, a large torque should be compensated. If the manipulator compensates for its torque when it is in contact with the tissue, it will rotate quickly and may harm human tissue or cause risky slippage in this case. We propose to detect this risk in the stable retraction. During the entire surgical process, we set a torque threshold $3.0N \cdot \text{mm}$.

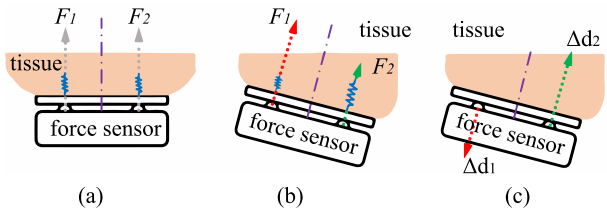

Fig. 3. Illustration of the contact correction by monitoring the torque applied on the force-sensing retractor. (a) An ideal contact has a balanced force distribution and small torque, while (b) the torque is noticeable if the orientation for retraction is not well aligned with the tissue. (c) We estimate the displacement at each signal point to correct the orientation.

Within the threshold, the minor torque compensation using PTC in the contact state is permitted. If the sensed torque exceeds the threshold, it is necessary to back to non-contact state and perform *Phase C*.

D. Active Retraction Angle Compensation

In the retraction compensation phase, we propose active retraction angle compensation (ARAC) to reduce the risk when the manipulator adjusts its orientation in the contact status. Instead of the compound motion of translation and rotation, we propose to retreat the retractor and decouple the rotational compensation in a non-contact state. We will use the information collected in the active retraction phase and compute it for the ARAC.

We treat human tissue as a non-linear soft object. Because the tissue deformation is almost static under stable retraction and the retraction in transoral surgery is usually not very fast for safety, we ignore the dynamic behavior of the soft tissue and use the force-displacement curve to characterize the physical model in this study. Specifically, we use a three orders polynomial to fit the force-deformation relationship

$$d = g(F) = a_0 + a_1F + a_2F^2 + a_3F^3 \tag{5}$$

where the deformation d refers to the retractor displacement after contact, and F is the net force in retraction. When the sensed force F_s exceeds $0.04\,N$, which is twice the minimal resolution of the force sensor, we regard the retractor is in contact with the tissues and start to record the displacement and the force. A polynomial fitting is run online to approximate the force-displacement curve. With the fitted curve $g(F)$, we estimate the deformation of each sensory signal $d_i = g(F_i), i = 1, 2, 3, 4$.

In the ideal contact state, we expect the force exerted on the retractor is balanced, i.e., the force signals sensed on the four contact points should be close. Assuming the tissues share the same physical model in the local contact region, it requires the displacement of each contact point to be equivalent. Therefore, the deformation to be compensated at each contact point is expected to be

$$\Delta d_i = \frac{\sum_{i=1}^{N} d_i}{N} - d_i. \tag{6}$$

Because we know the local coordinate of each sensory point as shown in Fig. 2, its position $\mathbf{p}_i$ under current configuration $\mathbf{q}$ is also available from forward kinematics. Then, we will search for a rotation R so that the displacement of each contact point is

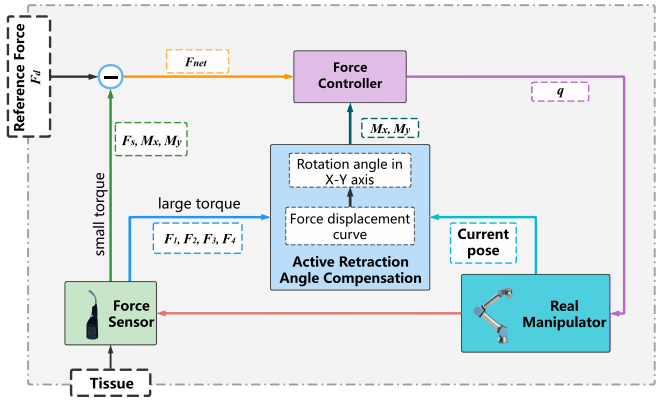

Fig. 4. Force control scheme diagram.

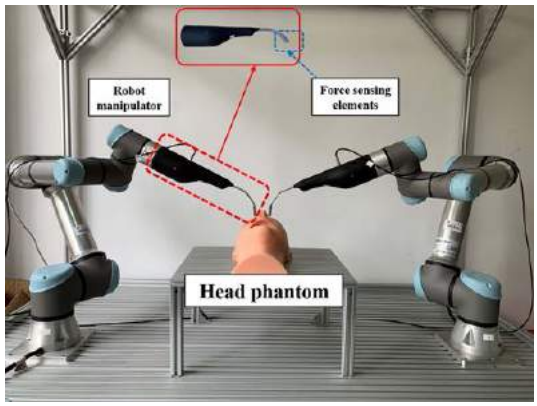

Fig. 5. The prototype of our robot-assisted retraction system and the experimental platform.

close to $\mathbf{p}_i + \Delta d_i \mathbf{n}$, where $\mathbf{n}$ is the normal of the blade region of the retractor. It corresponds to solve

$$\min_{R \in SO(3)} \sum_{i=1}^{4} \|R\mathbf{p}_i - (\mathbf{p}_i + \Delta d_i \mathbf{n})\|_2^2. \tag{7}$$

We use the Kabsch algorithm [33] to solve the above optimization problem for the optimal rotation.

The rotation matrix obtained from equation (7) is converted into a torque control signal and input into the controller. The manipulator will retreat from the contact status, update the orientation of the end-effector with the rotational matrix R and start another active retraction phase with the adjusted pose as the initialization. Note that we only use ARAC to quickly optimize for a large range of rotation angle compensation to avoid a substantial slipping contact. The final precise pose control is still achieved by PTC. The estimated rotation matrix R in ARAC does not have to be accurate. As long as the large rotation noticeably enhances the balance of the force signals, with the state from ARAC as initialization, our full controller will lead to a good contact configuration using PTC. If the contact is still with a large torque, we may take another phase C to refine the pose, similar to the trials of orientation adjustment in manual retraction. In practice, one iteration of the phase C is sufficient to correct the initial orientation in our experiments.

E. Final Control Scheme

The overall pipeline of the proposed method is illustrated in Fig. 4. The contact net-force F_s, torque M_x, M_y extracted from the four-way signals, single point forces F_1, F_2, F_3, F_4, and reference forces F_d are entered into the controller as the system inputs. The net force and the torques are entered into the force controller and work in *Phase R* and *Phase S*. Meanwhile, if the torque is high in *Phase S*, the contact forces on the four sensory points are directly input to the ARAC, which are applied in *Phase C*.

V. Experiments

A. Implementation Details

A prototype of the robot-assisted retraction system is implemented as the experimental platform, as shown in Fig. 5. The experimental platform consisted of two UR5 manipulators with two customized force-sensing retractors. We fixed the manipulators on the workbench spaced 1.3 m apart along the x-axis and connected them to a desktop. The system was controlled at 100 Hz in the Robot Operating System (ROS) running on Ubuntu18.04. The proportional and derivative gain were set as 0.1 and 0.3 for both the force and torque by default. The surgeons could trigger the retraction, switch the direct dragging mode or finetune the recommended force magnitude with a teach pendant. In our implementation, each retractor on the manipulator was controlled separately.

B. Experiments on Active Retraction

We first validate the robot-assisted retraction and perturbation resistance in *Phase R* with different contact objects. As shown in Fig. 6, sponge, silicone, and rigid models with three levels of softness were built to test the active retraction. A soft silicone model with rigid materials embedded inside was added to simulate the physiological structure. In addition, we test retracting tongue on a head phantom and inflate the hollow tongue to simulate tongue movement. The results in Fig. 6 show that the active retraction is able to accommodate materials of different levels of stiffness.

In order to verify that manipulators are able to mimic the manual retraction, we also compare our system with manual retraction. We collected the data from manual retraction in the above five scenarios. The retraction process was repeated 30 times by 3 surgeons. Optical markers were installed on the retractor and an optical tracking system (OptiTrack V120:Trio) was used to quantify the retraction length. We employed the manipulators to accomplish the same retraction process using the same retraction force. Statistics including maximum force, retraction length, and static force were collected in Table I. The retraction length here is the displacement of the retractor starting from its first contact with the tissue until its convergence to the

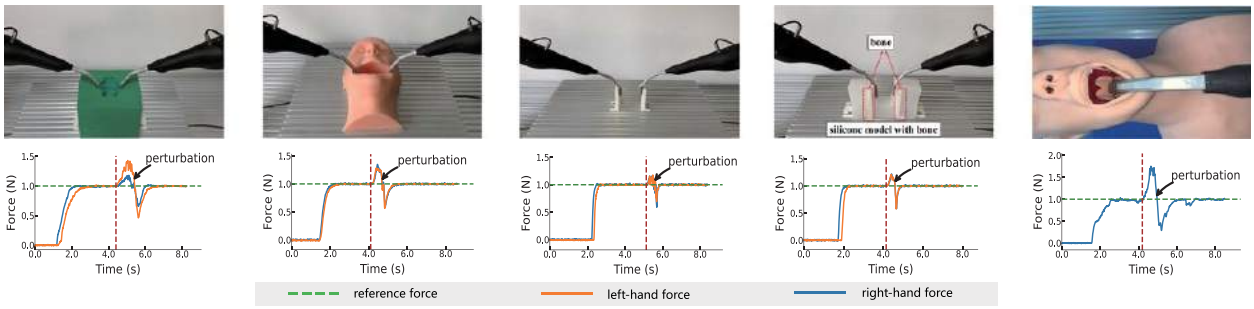

(a) sponge retraction (b) head model retraction (c) PLA retraction (d) silicone with bone retraction (e) tongue retraction

Fig. 6. Active retraction with five different objects. In each of test, we applied perturbations to test the ability to recover stability.

TABLE I
STATISTICS OF REPEATED EXPERIMENTS

operator	item	sponges	head model	PLA	silicone with bone	tongue
manual	maximum force (N)	1.673	1.828	3.044	2.217	2.368
	retraction time (s)	0.9±0.22	1.3±0.14	2.2±0.42	1.8±0.29	1.3±0.24
	retraction length (mm)	16.8±0.45	11.6±0.17	4.4±0.33	7.0±0.25	4.4±0.4
	static force (N) *	1.43±0.154	1.352±0.309	2.443±0.269	1.969±0.21	2.202±0.067
manipulator	maximum force (N)	1.445	1.357	2.461	1.982	2.227
	retraction time (s)	1.4±0.08	0.9±0.06	0.6±0.2	0.8±0.11	1.5±0.15
	retraction length (mm)	16.1±0.07	12.3±0.07	3.8±0.13	7.2±0.1	4.6±0.13
	static force (N) *	1.42±0.007	1.348±0.004	2.434±0.024	1.968±0.006	2.192±0.012

*$means \pm standard\ deviation$

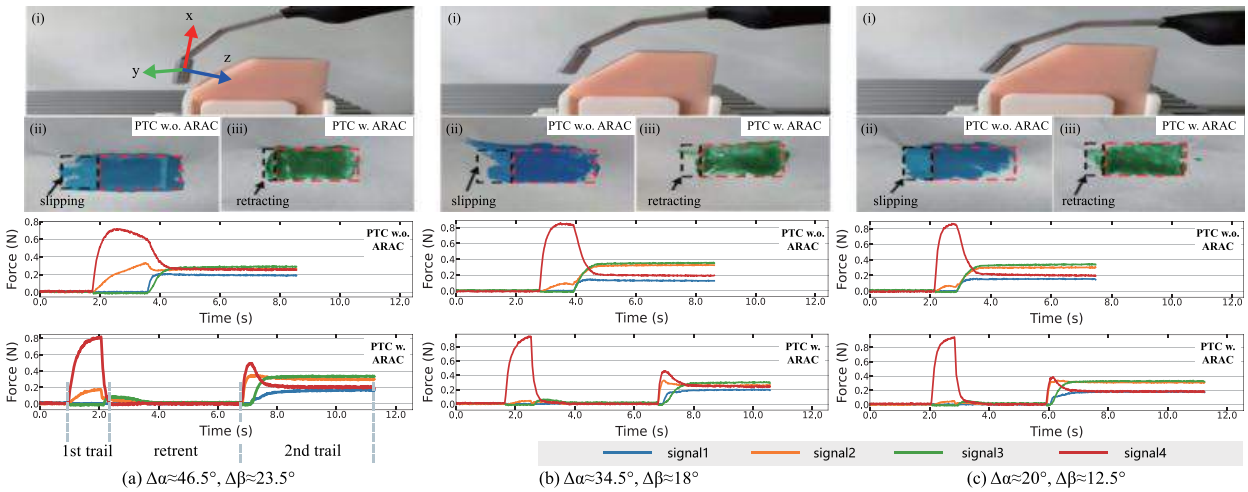

(a) Δα≈46.5°, Δβ≈23.5° (b) Δα≈34.5°, Δβ≈18° (c) Δα≈20°, Δβ≈12.5°

Fig. 7. Comparison of PTC without and with ARAC using three different initial poses. $\Delta\alpha$ and $\Delta\beta$ are the rotation angle offset about y-axis and x-axis. We show the initial pose (i), the contact region using PTC w.o ARAC (ii) and with ARAC (iii). The red areas are the contact surface, black areas illustrate the slipping footmark. The four-way force signals are also plotted below.

steady state. We list the average values of the retraction time and distance in the table for comparison. From the table, we observe similar behaviors of the robot-assisted retraction with the manual operation. Under the same static force, the manipulators have an exceptional accuracy range and the relative error of the stable retraction force does not exceed 11.8%.

C. Experiments on Active Retraction Angle Compensation

We also validated the active retraction angle compensation in our experiment. We deployed the PTC without and with ARAC to the platform. In order to demonstrate the slipping of the retractor on the contact surface more clearly, we used a 45° beveled silicone block for the experiment. At the beginning, we set three different initial poses for the contact state as shown in Fig. 7. In order to visualize the retractor slipping on the surface, we wet-painted all over the blade of the retractor. The area painted on the silicone block in contact would be larger when slippage occurs. As shown in the subfigures Fig. 7(ii)(iii), the slipping area is significantly reduced with ARAC. The maximum slipping areas of PTC without and with ARAC were $243.75\,\mathrm{mm}^2$ and $114.5\,\mathrm{mm}^2$ in the experiment.

TABLE II
STATISTICS OF STABLE RETRACTION EXPERIMENTS

item	head model	tongue	cadaver
perturbation range (mm)	4.3	3.5	\
maximum force (N)	1.013	1.033	1.223
static force (N) *	0.994±0.01	0.976±0.032	0.968±0.038
convergence time (s) *	0.45±0.12	1.15±0.23	0.73±0.16

*$means \pm standard\ deviation$

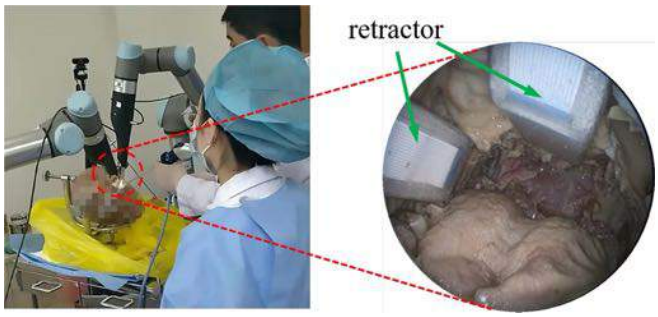

Fig. 8. Cadaveric experiment with our robot-assisted retraction.

We collected the four-way force signals of the retractor. As shown in Fig. 7, both methods enabled the force signals to converge to their equilibria. Since we set a lower bound for the torque compensation as described in IV-C, the force signals were not strictly equal to each other after stabilization. However, from the plots, we observed that after the orientation correction from ARAC, the retraction torque was reduced noticeably, e.g, in Fig. 7(a), the four-way force signals were more balanced after the ARAC step. We also computed the retraction torque in the test and it was reduced to $0.94\ N \cdot$ mm from $4.52N \cdot$ mm. A PTC step was then safe to rotate the manipulator to better hold the retractor. The torque convergence speed with ARAC of $0.98\ s$ was significantly faster than PTC w.o. ARAC of $2.14\ s$. Besides, the four-ways forces were not strictly equal after stabilization. This was caused by existence of considerable static friction, which was not favored in the stable retraction.

D. Experiments on Stable Retraction

We further verify the reliability and safety of the proposed method in the stable retraction. In the experiment, we randomly applied perturbations on the head phantom and tongue and then checked the physical indices. We simulated various perturbations generated by the surgeon operations during the actual surgery. The statistics including the range of perturbation, maximum force, static force, and convergence time were listed in Table II. The range of perturbation was measured using the same optical tracker.

We also tested our system on a cadaver model in Fig. 8. In the clinical scenario, the surgeons inserted an endoscope into the oral cavity to observe the surgical path in the cadaver, while the robot-assisted retraction helped expose the region of interest. In the cadaveric study, the perturbation was not measured due to the conflict of the optical tracking system and the actual cadaveric experiment. From the data, we could obtain that the control system was able to accomplish the task of tissue retraction on a cadaveric model and keeping it stable. The maximum force $1.223\ N$ was not high and did not damage the tissue. The stable retraction force was well kept near $1\ N$ as requested by the surgeon. The convergence time was about 0.73 s, which also met the surgeon's needs.

E. Discussion & Limitation

From the above experiments, we observe a robust performance of the robot-assisted retraction in random and unknown environments. The retractors response promptly and compliantly to avoid potential damage to human tissues. We have validated the control system on clinical cadavers and obtained satisfactory feedback. The surgeon found it flexible to use the system. He could decide when and where to retract. The manipulators reliably assisted the retraction task in the cadaveric experiment. The surgeon also suggested to vary the range of the sensor and the shape of the retractor. In this way, the system can be used for more surgical procedures such as thyroid gland surgery or knee arthroplasty.

In this study, the success of the proposed robot-assisted retraction relies on the force-sensing unit of the system, which is yet to be improved in the future. We have not sensed the friction on the contact surface and do not precisely measure the retractor slipping. Although ARAC reduces slippage, the slippage cannot be eliminated completely. We will improve the force sensing structure to support slipping detection at the distal end and the contact surfaces tracking.

In this work, we use a simple physical model to test our system with simulated tongue motion. It is appropriate to assume that patients are cooperative and no active tongue motion will be taken in the surgery. But it is interesting to further look into the cases with challenging tongue motions and we will work on high-fidelity physical tongue simulators or clinical experiments to test our system. In the cadaveric experiment, we did not collect data on the perturbation distance. In the future, we expect to switch to other measurement methods, e.g, electromagnetic sensors, to observe the displacement inside the oral cavity.

As two manipulators are working in the narrow oral cavity, the rotation angle compensation may cause collisions between the two manipulators. In future work, we will consider compensating the offset of the ARAC and deploying collision avoidance. We also hope to model tissues accurately and create a database of tissue stiffness. In this way, the control system may autonomously identify and adaptively recommend the retraction force online. Furthermore, we intend for this system to be used clinically to support manual transoral surgeries.

VI. CONCLUSION

We propose a human-robot collaboration system to facilitate the tissue retraction task for transoral surgery. With our system, the surgeon only needs to roughly align the retractor to indicate target contact surfaces and retraction magnitude, and the robot will automatically adjust its motion to safely retract the tissues for the surgeon in a natural way. In the absence of slip sensing, we use a combination of ARAC and PTC to reduce slippage

on the contact surface. We experiment with different situations and report the statistics of the robot. The results show that the retractor is safely held and quickly acted under unknown perturbations, which shows its potential in assisting the surgeon in an open surgical environment.

Although we find that our control scheme works quite well in the surgical application, we could further improve the interaction controller or develop a bimanual shared control for better performance. To further facilitate the surgeons, we will adapt our system to retractors with different forms or retractions for other types of surgery. In this work, we validate the proposed solution with a physical phantom. With the robust performance of the system, we are ready to run more animal and clinical experiments in the future.

REFERENCES

[1] P. R. Steele, J. F. Curran, and R. E. Mountain, "Current and future practices in surgical retraction," *Surgeon*, vol. 11, no. 6, pp. 330–337, Dec. 2013, doi: 10.1016/j.surge.2013.06.004, PMID: 23932799.

[2] L. Çetin, E. Temiz, and E. Kuralay, "Retractor in retractor technique," *Indian J. Thoracic Cardiovasc. Surg.*, vol. 35, pp. 264–265, 2019.

[3] I. Alkatout, "An atraumatic retractor for interdisciplinary use in conventional laparoscopy and robotic surgery," *Minimally Invasive Ther. Allied Technol.*, vol. 27, pp. 265–271, 2018.

[4] P. E. Dupont et al., "A decade retrospective of medical robotics research from 2010 to 2020," *Sci. Robot.*, vol. 6, no. 60, Nov. 2021, Art. no. eabi8017.

[5] A. Attanasio et al., "Autonomous tissue retraction in robotic assisted minimally invasive surgery–A feasibility study," *IEEE Robot. Automat. Lett.*, vol. 5, no. 4, pp. 6528–6535, Oct. 2020.

[6] T. D. Nagy, M. Takács, I. J. Rudas, and T. Haidegger, "Surgical subtask automation–Soft tissue retraction," in *Proc. IEEE 16th World Symp. Appl. Mach. Intell. Inform.*, 2018, pp. 55–60.

[7] A. Pore et al., "Safe reinforcement learning using formal verification for tissue retraction in autonomous robotic-assisted surgery," in *Proc. IEEE/RSJ Int. Conf. Intell. Robots Syst.*, 2021, pp. 4025–4031.

[8] A. Pore, E. Tagliabue, M. Piccinelli, D. Dall'Alba, A. Casals, and P. Fiorini, "Learning from demonstrations for autonomous soft-tissue retraction," in *Proc. IEEE Int. Symp. Med. Robot.*, 2021, pp. 1–7.

[9] L. Zhu et al., "A force-sensing retractor for robot-assisted transoral surgery," *Int. J. Comput. Assist. Radiol. Surg.*, vol. 17, pp. 2001–2010, 2022, doi: 10.1007/s11548-022-02677-1.

[10] H. Yin, A. Varava, and D. Kragic, "Modeling, learning, perception, and control methods for deformable object manipulation," *Sci. Robot.*, vol. 6, 2021, Art. no. eabd8803.

[11] P. Boonvisut, R. Jackson, and M. C. Çavuşoğlu, "Estimation of soft tissue mechanical parameters from robotic manipulation data," in *Proc. IEEE Int. Conf. Robot. Automat.*, 2012, pp. 4667–4674, doi: 10.1109/ICRA.2012.6225071.

[12] M. Azad, V. Ortenzi, H.-C. Lin, E. Rueckert, and M. Mistry, "Model estimation and control of compliant contact normal force," in *Proc. IEEE-RAS 16th Int. Conf. Humanoid Robots*, 2016, pp. 442–447, doi: 10.1109/HUMANOIDS.2016.7803313.

[13] F. Liu, Z. Li, Y. Han, J. Lu, F. Richter, and M. C. Yip, "Real-to-sim registration of deformable soft tissue with position-based dynamics for surgical robot autonomy," in *Proc. IEEE Int. Conf. Robot. Automat.*, 2021, pp. 12328–12334, doi: 10.1109/ICRA48506.2021.9561177.

[14] P. Hasskamp et al., "First use of a new retractor in transoral robotic surgery (TORS)," *Eur. Arch. Oto-Rhino- Laryngology*, vol. 273, no. 7, pp. 1913–1917, 2016.

[15] B. S. Peters et al., "Review of emerging surgical robotic technology," *Surg. Endoscopy*, vol. 32, no. 4, pp. 1636–1655, 2018.

[16] N. T. Burkhard, M. R. Cutkosky, and J. R. Steger, "Slip sensing for intelligent, improved grasping and retraction in robot-assisted surgery," *IEEE Robot. Automat. Lett.*, vol. 3, no. 4, pp. 4148–4155, Oct. 2018.

[17] T. Watanabe et al., "Force-sensing silicone retractor for attachment to surgical suction pipes," *Sensors*, vol. 16, no. 7, 2016, Art. no. 1133.

[18] I. Nigicser, M. Oldfield, and T. Haidegger, "Stability and retraction force verification of a new retractor design for minimally invasive surgery," in *Proc. IEEE 25th Int. Conf. Intell. Eng. Syst.*, 2021, pp. 183–188.

[19] A. Cavallo et al., "A soft retraction system for surgery based on ferromagnetic materials and Granular jamming," *Soft Robot.*, vol. 6, no. 2, pp. 161–173, 2019.

[20] B. K. Poulose et al., "Human vs robotic organ retraction during laparoscopic Nissen fundoplication," *Surg. Endoscopy*, vol. 13, no. 5, pp. 461–465, 1999.

[21] S. Patil and R. Alterovitz, "Toward automated tissue retraction in robot-assisted surgery," in *Proc. IEEE Int. Conf. Robot. Automat.*, 2010, pp. 2088–2094.

[22] D. Meli, E. Tagliabue, D. Dall'Alba, and P. Fiorini, "Autonomous tissue retraction with a biomechanically informed logic based framework," in *Proc. IEEE Int. Symp. Med. Robot.*, 2021, pp. 1–7.

[23] S. Scherzinger, A. Roennau, and R. Dillmann, "Forward dynamics compliance control (FDCC): A new approach to cartesian compliance for robotic manipulators," in *Proc. IEEE/RSJ Int. Conf. Intell. Robots Syst.*, 2017, pp. 4568–4575.

[24] C. Ott, R. Mukherjee, and Y. Nakamura, "Unified impedance and admittance control," in *Proc. IEEE Int. Conf. Robot. Automat.*, 2010, pp. 554–561.

[25] C. Liang, S. Bhasin, K. Dupree, and W. E. Dixon, "A force limiting adaptive controller for a robotic system undergoing a noncontact-to-contact transition," *IEEE Trans. Control Syst. Technol.*, vol. 17, no. 6, pp. 1330–1341, Nov. 2009.

[26] S. A. Khader, H. Yin, P. Falco, and D. Kragic, "Stability-guaranteed reinforcement learning for contact-rich manipulation," *IEEE Robot. Automat. Lett.*, vol. 6, no. 1, pp. 1–8, Jan. 2021, doi: 10.1109/LRA.2020.3028529.

[27] D. Mitrovic, S. Klanke, and S. Vijayakumar, "Learning impedance control of antagonistic systems based on stochastic optimization principles," *Int. J. Robot. Res.* vol. 30, no. 5, pp. 556–573, 2011.

[28] N. Dehio and A. Kheddar, "Robot-safe impacts with soft contacts based on learned deformations," in *Proc. IEEE Int. Conf. Robot. Automat.*, 2021, pp. 1357–1363.

[29] M. Bednarczyk, H. Omran, and B. Bayle, "Model predictive impedance control," in *Proc. IEEE Int. Conf. Robot. Automat.*, 2020, pp. 4702–4708.

[30] P. Long, W. Khalil, and P. Martinet, "Force/vision control for robotic cutting of soft materials," in *Proc. IEEE/RSJ Int. Conf. Intell. Robots Syst.*, 2014, pp. 4716–4721.

[31] Y. Guo, X. Jiang, and Y. Liu, "Deformation control of a deformable object based on visual and tactile feedback," in *Proc. IEEE/RSJ Int. Conf. Intell. Robots Syst.*, 2021, pp. 675–681.

[32] D. Ma, S. Dong, and A. Rodriguez, "Extrinsic contact sensing with relative-motion tracking from distributed tactile measurements," in *Proc. IEEE Int. Conf. Robot. Automat.*, 2021, pp. 11262–11268.

[33] W. Kabsch, "A solution for the best rotation to relate two sets of vectors," *Acta Crystallographica Sect. A*, vol. 3, no. 2, pp. 922–923, 1976.